# Sudden Interchannel Interaction in the Tl 6*p* Ionization above the 5*d* Threshold

G. Prümper,[1] B. Zimmermann,[1] B. Langer,[2] J. Viefhaus,[1] R. Hentges,[1] N. A. Cherepkov,[1,3]
B. Schmidtke,[4] M. Drescher,[4] U. Heinzmann,[4] U. Becker,[1] and H. Kleinpoppen[5]

[1]*Fritz-Haber-Institut der Max-Planck-Gesellschaft, D-14195 Berlin, Germany*
[2]*Max-Born-Institut, D-12489 Berlin, Germany*
[3]*State University of Aerospace Instrumentation, 190000 St. Petersburg, Russia*
[4]*Fakultät für Physik, Universität Bielefeld, D-33615 Bielefeld, Germany*
[5]*University of Stirling, Atomic Physics Unit, Stirling FK9 4LA, United Kingdom*
(Received 11 February 2000; revised manuscript received 15 June 2000)

The linear magnetic dichroism in the angular distribution of Tl 5*d* and 6*p* photoelectrons and their dynamical spin polarization have been measured between $h\nu = 30$ and 50 eV. In contrast to the Xe 5*p* photoionization at the 4*d* threshold, our results show that above the Tl 5*d* threshold strong interchannel coupling effects induce a sudden increase in the asymptotic phase difference of the *s* and *d* waves for the Tl 6*p* ionization. This shows that the valence excitation is different for resonant (Xe 4*d*) and nonresonant (Tl 5*d*) excitation from subvalence shells.

PACS numbers: 32.80.Fb

Strong photoionization channels may significantly affect the behavior of weaker channels due to the coupling by electron correlation. The showcase example for such a situation is the Xe 5*p* photoionization in the vicinity of the 4*d* shape resonance [1–3]. The latter effect can be understood as the polarization of the atom, induced by the strong photoionization channel, giving rise to enhanced electron emission in the weaker channel.

Interchannel coupling has a pronounced impact on the phase shift between the two outgoing photoelectron waves $\epsilon_{l+1}$ and $\epsilon_{l-1}$ [4]. This phase effect occurs very slowly in the Xe 5*p* case, showing little interchannel coupling effect on the phase shift between the two outgoing waves $\epsilon s$ and $\epsilon d$ just above the 4*d* threshold, due to the delayed onset of the 4*d* photoionization. It basically develops with the appearance of the shape resonance in the 4*d* channel inducing a similar but less pronounced change in the phase shift of the 5*p* channel. This smooth variation of all photoionization parameters makes the whole process behave like a resonance in the sense of a broadband autoionizing resonance. In contrast to this, recent studies of the photoionization of Ne 2*p* indicate a sudden onset of the interchannel coupling at threshold of the interacting 1*s* channel [5]. The phase shift change exhibited in the Ne 2*p* channel in the region of the 1*s* threshold is small compared with the change of the Xe 5*p* electron in the region of the 4*d* threshold. Additionally the two types of interchannel coupling, resonant and nonresonant, differ qualitatively dramatically in the phase dependent angular distributions and theoretically derived phase shifts. This is shown in Fig. 1 which compares Xe 5*p* data of Fig. 20 of [3] with the recent Ne 2*p* measurements of [5]. However, the *np* photoionization of Ne and Xe are quite different with respect to the orbital angular momentum of the new interacting channel. This makes it difficult to generalize the conclusions drawn from such a comparison. Therefore, the question arises if in general the coupling between two channels appears suddenly above threshold or if the xenon case, where the coupling is mediated by a resonance feature in the continuum of the stronger channel, is the more common one.

In order to answer this question, the coupling between two subshell photoionization channels that have, on the one hand, nonzero orbital angular momenta (as in Xe 4*d*) but also a clear onset of the new channel (as in Ne 1*s* and many other cases) should be studied. For simplicity only two channels should be involved. Such a case is the Tl 6*p* photoionization in the vicinity of the 5*d* threshold.

We used the linear magnetic dichroism in the angular distribution (LMDAD) of photoelectrons ejected from polarized atoms [6–8], the dynamical spin polarization $P_{\mathrm{dyn}}$, and the angular distribution of photoelectrons ejected from unpolarized atoms to perform a partial wave analysis for

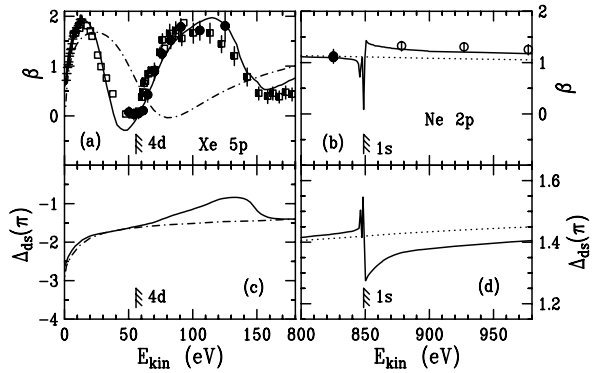


FIG. 1. Xe 5*p* (a) and Ne 2*p* (b) photoelectron angular distributions [3,5] along with the corresponding phase shifts between the $\epsilon d$- and $\epsilon s$-partial waves [4] in the vicinity of the Xe 4*d* (c) and Ne 1*s* (d) thresholds, respectively. The solid curves represent RPAE calculations with full interchannel coupling, whereas the dash-dotted line neglects the Xe 4*d* coupling and the dotted line neglects the 1*s* coupling.

 0031-9007/00/85(24)/5074(4)$15.00 

the reactions (1) and (2)

$$\mathrm{Tl}\ 5d^{10}6s^2 6p(^2P_{1/2}) + h\nu \rightarrow \mathrm{Tl}^+\ 5d^9(^2D_{3/2}) \times 6s^2 6p(^2P_{1/2}) \times (J = 1) + e^- \quad (1)$$

$$\mathrm{Tl}\ 5d^{10}6s^2 6p(^2P_{1/2}) + h\nu \rightarrow \mathrm{Tl}^+\ 5d^{10}6s^2 + e^- . \quad (2)$$

Because of the coupling between the polarized Tl $6p$ electron and the $5d$ hole created in reaction (1), dichroism effects can also be observed in the multiplet of an unpolarized closed shell [9] like the $5d$ shell. For atoms with a total angular momentum $J = \frac{1}{2}$ in the initial state, the intensity of the photoelectrons in the detection plane perpendicular to the propagation of the light is given by Eqs. (3) and (4) with $I_{\uparrow\uparrow}$ and $I_{\uparrow\downarrow}$ being the count rates for the atomic polarization $\vec{A}$ parallel and antiparallel to the propagation of the light $\vec{k}$, respectively.

$$I_{\uparrow\uparrow}(\Theta) = I_0\left\{1 + \frac{\beta}{4}[1 + 3P_1\cos(2\Theta)] + A_{10}P_1\beta'\sin(2\Theta)\right\}, \quad (3)$$

$$I_{\uparrow\downarrow}(\Theta) = I_0\left\{1 + \frac{\beta}{4}[1 + 3P_1\cos(2\Theta)] - A_{10}P_1\beta'\sin(2\Theta)\right\}. \quad (4)$$

$I_0$ describes the total electron intensity which is proportional to the target density, the acceptance angle, the light intensity, the cross section, and the detection efficiency. $\Theta$ is the angle between the detection direction and the electric vector of the light. $A_{10}$ is the degree of the atomic orientation, and $P_1$ the degree of linear polarization of light. The other Stokes polarization parameters $P_2$ and $P_3$ are assumed to be zero. This has been confirmed in LMDAD measurements for oxygen [8]. For the two reactions (1) and (2) $\beta$ is given by [10]

$$\beta_{5d} = \frac{2 + 12\gamma_{fp}^2 - 36\gamma_{fp}\cos(\Delta_{fp})}{5(2 + 3\gamma_{fp}^2)}, \quad (5)$$

$$\beta_{6p} = \frac{2\gamma_{ds}^2 - 4\gamma_{ds}\cos(\Delta_{ds})}{1 + 2\gamma_{ds}^2}, \quad (6)$$

and $\gamma$ is defined by the ratio of the radial dipole matrix elements:

$$\gamma_{fp} = \frac{r_f}{r_p}, \qquad \gamma_{ds} = \frac{r_d}{r_s}, \qquad r_{l\pm1} = \int_0^\infty P^*_{\epsilon l\pm1}(r) r P_{nl}(r)\, dr . \quad (7)$$

$P_{nl}(r)$ is the radial part of the wave function of the bound electron and $P_{\epsilon l\pm1}(r)$ is that of the outgoing photoelectron waves. $\Delta_{fp}$ and $\Delta_{ds}$ are the differences in their asymptotic phase shifts. These equations use the following definitions for the asymptotic phase shifts of the partial waves: the total asymptotic phase shift is $\Delta_{l+1,l-1} = \sigma_{l+1} + \delta_{l+1} - \sigma_{l-1} - \delta_{l-1}$. The Coulombic phase is defined by $\sigma_l = \arg[\Gamma(l + 1 - \frac{i}{E_{\mathrm{kin}}/R_\infty})]$ with $R_\infty = 13.605\,67$ eV. So the Coulombic phase difference $\sigma_{l+1} - \sigma_{l-1}$ is $\pi$ at the threshold and approaches $2\pi$ at high kinetic energies. With these definitions Seaton's theorem [11] can be used to determine the intrinsic phase difference $\delta_{l+1} - \delta_{l-1}$ at the threshold:

$$\lim_{n\rightarrow\infty}\pi(\mu_{n,l+1} - \mu_{n,l-1}) = \lim_{E_{\mathrm{kin}}\rightarrow0}\delta_{l+1} - \delta_{l-1} . \quad (8)$$

$\beta'$ in Eqs. (3) and (4) describes the magnetic dichroism [12]. The value of $\beta'$ depends additionally on the angular momenta of the ionic final state. For the two reactions (1) and (2) the parameter $\beta'$ is given by

$$\text{reaction (1): } \beta' = \frac{9}{2}\frac{\gamma_{fp}}{2 + 3\gamma_{fp}^2}\sin(\Delta_{fp}), \quad (9)$$

$$\text{reaction (2): } \beta' = 3\frac{\gamma_{ds}}{1 + 2\gamma_{ds}^2}\sin(\Delta_{ds}). \quad (10)$$

To keep the model as simple as possible, we neglected the mixing of the states of the $5d$ multiplet, and the $\beta'$ parameter in Eq. (9) is calculated assuming pure $jj$ coupling for the ionic state. An analysis of the configuration mixing coefficients of the $5d$ multiplet [13] shows that the dichroism effects are not affected significantly by the intermediate coupling. The maximum dichroism effect, i.e., the maximum difference between the intensities $I_{\uparrow\uparrow}$ and $I_{\uparrow\downarrow}$ is observed for $\Theta = 45°$ [see Eqs. (3) and (4)]. To eliminate the unknown absolute intensity $I_0$ the asymmetry is measured. For $\Theta = 45°$ the asymmetry is

$$\text{LMDAD asymmetry} = \frac{(I_{\uparrow\uparrow} - I_{\uparrow\downarrow})}{(I_{\uparrow\uparrow} + I_{\uparrow\downarrow})} = \frac{A_{10}P_1\beta'}{1 + \frac{\beta}{4}}. \quad (11)$$

Alternatively the dynamical spin polarization $P_{\mathrm{dyn}}$ can be measured with a beam of unpolarized atoms:

$$(1): P_{\mathrm{dyn}} = -\frac{15\gamma_{fp}\sin(\Delta_{fp})}{7 - 6\gamma_{fp}\cos(\Delta_{fp}) + 12\gamma_{fp}^2}, \quad (12)$$

$$(2): P_{\mathrm{dyn}} = -\frac{6\gamma_{ds}\sin(\Delta_{ds})}{2 - 2\gamma_{ds}\cos(\Delta_{ds}) + 5\gamma_{ds}^2}. \quad (13)$$

The LMDAD asymmetry and the dynamical spin polarization are closely related. Equations (6) to (13) yield for reactions (1) and (2):

$$\text{LMDAD asymmetry} = -A_{10}P_1P_{\mathrm{dyn}} . \quad (14)$$

For the measurement of $P_{\mathrm{dyn}}$ the Mott-scattering target is positioned at $\Theta = 45°$ and the detectors measure the spin component parallel to $\vec{k}$. The details of this technique are explained in [14].

The experimental setup for the LMDAD asymmetry measurement is explained in [8] and [15]. We will give

only a brief description: An electron impact oven evaporates the Tl, a hexapole magnet (gap 3 mm, pole tip field strength 760 mT, length 175 mm) selects one of the two magnetic sublevels of the $2P_{1/2}$ ground state. A weak magnetic guiding field ($<2\mu T$) is applied, defining the direction of atomic polarization $\vec{A}$ at the position where the atomic beam intersects the ionizing radiation. The degree of atomic polarization $A_{10}$ is defined by the population numbers of the magnetic sublevels $g_{M_J}$ [16]: $A_{10} = g_{M_J=+1/2} - g_{M_J=-1/2}$. For Tl an atomic polarization of $A_{10} = 0.33 \pm 0.03$ was determined with a Monte Carlo simulation of the atomic beam. This simulation takes into account the hyperfine interaction, the variation of the magnetic moment as a function of the magnetic field, the effect of possible misalignment, and the thermal velocity distribution of the metal vapor. The experiment was performed at the BESSY U1 TGM5 and TGM6 undulator beam lines (our typical operation parameters were $h\nu = 30$–$50$ eV, linear polarization $P_1 \geqslant 0.95$, flux $10^{14}$–$10^{13}$ photons/s), and the HASYLAB BW3 undulator beam line (typical operation parameters $h\nu = 30$–$150$ eV, $P_1 \geqslant 0.97$, $10^{13}$–$10^{11}$ photons/s).

With two measured quantities—either $\beta$ and the LMDAD asymmetry or $\beta$ and $P_{\mathrm{dyn}}$—a partial wave analysis yields the ratio of the radial dipole matrix elements $\gamma$ and the asymptotic phase difference $\Delta$. The solution is not unique, and one of the solutions for the pair $(\gamma, \Delta)$ has to be rejected after comparison with theory.

Two methods, with different levels of sophistication, have been used to determine these dynamical parameters theoretically, a frozen core Hartree-Fock (HF) calculation and a random phase approximation with exchange (RPAE) calculation [17,18]. The latter includes the correlation of the photoelectron and the residual electrons.

Figure 2 shows HF and RPAE results for the $5d$ shell. In this energy region the linear magnetic dichroism in the angular distribution of the photoelectrons changes sign, as the phase difference between the $f$ and $p$ waves goes through a multiple of $\pi$. A similar behavior of the phase difference of the $p$ and $f$ waves was found for mercury by Schönhense and co-workers [19]. They observed a smooth rise of the phase difference of $\approx 1.5\pi$ from threshold to a kinetic energy of 30 eV for the $5d$ ionization. The phase difference values for the Hg $5d$ ionization are very similar to the Tl $5d$ ionization. They differ by $2\pi$ as the Hg phase difference in [19] was not matched to the corresponding quantum defects of $\approx -3.2$ (calculated from [20]). The results of the RPAE calculation agree well with the observations of the $[5d^9(^2D_{3/2})6s^2 6p(^2P_{1/2})\ J = 1]$ line. The differences between the HF and RPAE calculations are small, but nevertheless the measurements favor the RPAE results. For reaction (1) the $6p$ electron is treated as a spectator. The measurements are in good agreement with the RPAE results, and consequently the partial wave analysis has to agree with the calculated values of $\gamma_{fp}$ and $\Delta_{fp}$. The second solutions for the partial wave decomposition are shown as open circles in Fig. 2.

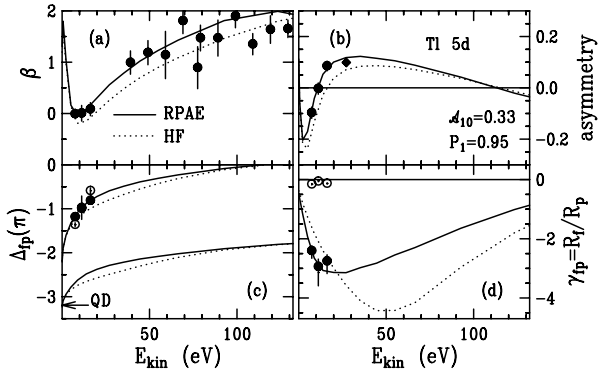


FIG. 2. The angular distribution of photoelectrons of unpolarized and polarized atoms are shown in (a) and (b) in the form of the $\beta$ parameter and the asymmetry defined by Eq. (11). A measurement of the dynamical spin polarization has been included in the diagram as a diamond using Eq. (14). Observations of $\beta$ and the asymmetry are transformed into the ratio of the dipole matrix elements $\gamma_{fp}$ (d) and the asymptotic phase difference $\Delta_{fp}$ (c). This transformation is not unique but the comparison with theory (solid and dotted lines) allows one to reject one of the two solutions (open circles). The lower curves in (c) represent the phase differences without the Coulombic phase shifts. They match the difference of the quantum defects (QD) at the ionization threshold. The value of $-3.2$ was determined from [21].

In order to describe the continuum coupling effects of the Tl $6p$ ionization, the interaction of an electron emitted from the $5d$ shell with the bound $6p$ electron must be included. The RPAE method has been used only for atoms with one open shell so far. We had to neglect the coupling of the $5d$ hole and the $6p$ electron, and we included the RPAE correlations between the $5d$ and $6p$ ionization channels. The $6p$ cross section is much smaller than that for the $5d$ ionization. Figure 3 shows the HF and the RPAE results for the Tl $5d$ and $6p$ cross section. The RPAE curve of the Tl $6p$ cross section stops its exponential decay at the $5d$ threshold due to interchannel

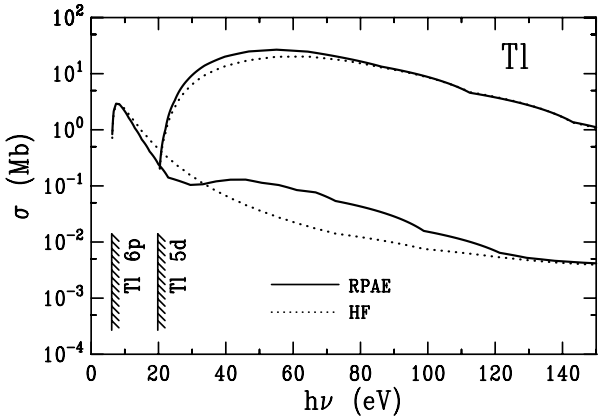


FIG. 3. RPAE and HF calculations of the Tl $5d$ and Tl $6p$ lines. The Tl $6p$ and Tl $5d$ thresholds are at 6.11 and 19.79 eV, respectively [20].

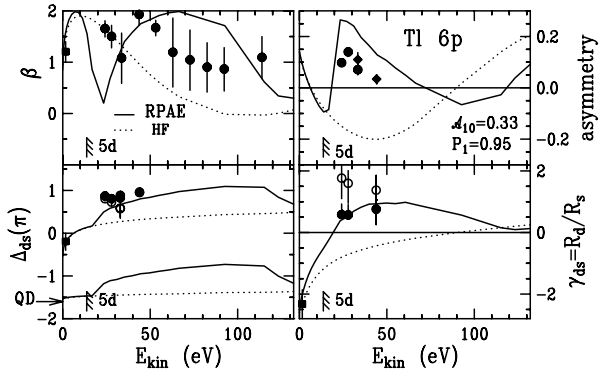


FIG. 4. Observations of the angular distribution of polarized atoms are transformed into the ratio of the dipole matrix elements $\gamma$ and the asymptotic phase difference $\Delta_{ds}$. Open and closed circles are as in Fig. 2. The measurements of the dynamical spin polarization have been included in the diagram as diamonds using Eq. (14). The low energy data point is taken from the nonresonant data points in [22]. The lower curves in the diagram for the phase difference represent the phase differences without the Coulombic phase shifts. They match the difference of the quantum defects (QD )at the ionization threshold. The value of $-1.6$ was determined from [20].

coupling contributions. Figure 4 shows a sudden phase increase in the RPAE curve with respect to the HF calculation right at the $5d$ threshold. The ratio of the matrix elements also differs for the two calculations, but there is no visible threshold effect. The comparison with the experimental data rules out the HF results that yield the wrong sign of the LMDAD asymmetry. The results of the partial wave analysis indicate that the phase in the RPAE calculation is still too low to describe the observables correctly. We assign this discrepancy to the approximation discussed above.

The sudden rise of the asymptotic phase difference may be a peculiarity in the coupling of the continuum channels in Tl. However, the comparison with Ne [5] suggests another explanation. In the case of Xe the overlap of the uncollapsed $4d \rightarrow \varepsilon f$ wave function with the $5p$ photoionization channel is so small at threshold that interchannel interactions become ineffective. This means that the Xe case with the shape resonance, although considered as a showcase example for interchannel coupling behavior, represents rather a resonancelike behavior with a smooth variation of the phase shift. The more common case is the cross section driven sudden phase jump as seen in Ne and now corroborated for the case of Tl, a system with Xe-like subshells. This points to a more general tendency for valence photoionization to follow the behavior of the dominant inner shell which determines the rate of change of cross section and phase shift.

In summary, we have shown that strong interchannel coupling between the Tl $6p$ and $5d$ subshells occurs suddenly above the $5d$ threshold, in marked contrast to the phase shift behavior of the Xe $5p$ and $4p$ subshells. This coupling gives rise to an abrupt change in the phase shift between the $s$ and $d$ waves of the Tl $6p$ ionization indicating a different valence photoionization in the presence of subvalence resonant and nonresonant behavior.

H. K. acknowledges the support of the European Union and the Leverhulme Trust Company (London). N. A. C. acknowledges the Max-Planck-Society for financial support and the Fritz-Haber-Institut for hospitality. This work was supported by the Deutsche Forschungsgemeinschaft.

[1] M. Ya. Amusia *et al.,* Sov. Phys. JETP **39**, 752 (1974).
[2] J. B. West *et al.,* J. Phys. B **9**, 407 (1976).
[3] U. Becker and D. A. Shirley, in *VUV- and Soft X-Ray Photoionization,* edited by U. Becker and D. A. Shirley (Plenum Press, New York, 1996).
[4] B. Zimmermann *et al.,* in *Proceedings of the 21st International Conference on the Physics of Electronic and Atomic Collisions (ICPEAC), Sendai, Japan, 1999, Abstracts of Contributed Papers,* edited by Y. Itikawa, K. Okuno, H. Tanaka, A. Yagishita, and M. Matsuzawa (Local Organizing Committee of XXI ICPEAC, Tokyo, 1999), Vol. I, p. 41.
[5] E. W. B. Dias *et al.,* Phys. Rev. Lett. **78**, 4553 (1997); O. Hemmers *et al.,* J. Phys. B **30**, L727 (1997).
[6] H. Klar and H. Kleinpoppen, J. Phys. B **15**, 933 (1982).
[7] N. A. Cherepkov, V. V. Kuznetsov, and V. A. Verbitskii, J. Phys. B **28**, 1221 (1995).
[8] O. Plotzke *et al.,* Phys. Rev. Lett. **77**, 2642 (1996).
[9] A. von dem Borne *et al.,* Phys. Rev. Lett. **78**, 4019 (1997).
[10] J. W. Cooper and R. N. Zare, J. Chem. Phys. **48**, 942 (1968); **49**, 4252(E) (1969).
[11] M. J. Seaton, Rep. Prog. Phys. **46**, 167 (1983).
[12] In [8] the parameter $\beta'$ is defined differently. The product $A_{10}\beta'$ in this paper is represented in [8] by $c_2\beta'$.
[13] R. D. Cowan, *The Theory of Atomic Structure and Spectra* (University of California Press, Berkeley, Los Angeles, London, 1981). We performed the calculation using the codes RCN and RCG.
[14] G. Snell *et al.,* Phys. Rev. Lett. **76**, 3923 (1996).
[15] G. Prümper *et al.,* Europhys. Lett. **38**, 19 (1997).
[16] K. Blum, *Density Matrix Theory and Applications* (Plenum Press, New York, 1981).
[17] M. Ya. Amusia and N. A. Cherepkov, Case Stud. At. Phys. **5**, 47 (1975).
[18] M. Ya. Amusia and L. V. Chernysheva, *Computation of Atomic Processes* (Institute of Physics Publishing, Bristol, Philadelphia, 1997).
[19] G. Schönhense and U. Heinzmann, Phys. Rev. A **29**, 987 (1984).
[20] C. E. Moore, Atomic Energy Levels Vol. 1, Circular of the National Bureau of Standards No. 467 (1949).
[21] J. P. Connerade *et al.,* Proc. R. Soc. London A **350**, 47 (1976).
[22] M. Müller *et al.,* J. Phys. B **23**, 2267 (1990).